Expert Systems with Applications 38 (2011) 12514–12520

Contents lists available at ScienceDirect

Expert Systems with Applications

journal homepage: www.elsevier.com/locate/eswa

Ant colony optimization for wavelet-based image interpolation using a three-component exponential mixture model

Jing Tian [a,*], Lihong Ma [b], Weiyu Yu [c]

[a] School of Computer Science and Technology, Wuhan University of Science and Technology, Wuhan 430081, PR China
[b] Guangdong Key Lab. of Wireless Network and Terminal, School of Electronic and Information Engineering, South China University of Technology, Guangzhou 510641, PR China
[c] School of Electronic and Information Engineering, South China University of Technology, Guangzhou 510641, PR China

ARTICLE INFO

Keywords:
Image interpolation
Ant colony optimization

ABSTRACT

Wavelet-based image interpolation typically treats the input image as the low frequency subbands of an unknown wavelet-transformed high-resolution image, and then produces the unknown high-resolution image by estimating the wavelet coefficients of the high frequency subbands. For that, a new approach is proposed in this paper, the contribution of which are twofold. First, unlike that the conventional *Gaussian mixture* (GM) model only exploits the magnitude information of the wavelet coefficients, a *three-component exponential mixture* (TCEM) model is proposed in this paper to investigate both the magnitude information and the sign information of the wavelet coefficients. The proposed TCEM model consists of a Gaussian component, a positive exponential component and a negative exponential component. Second, to address the parameter estimation challenge of the proposed TCEM model, the *ant colony optimization* (ACO) technique is exploited in this paper to classify the wavelet coefficients into one of three components of the proposed TCEM model for estimating their parameters. Experiments are conducted to demonstrate that the proposed approach outperform a number of approaches developed in the literature.

1. Introduction

Wavelet-based techniques have been widely used for performing image interpolation. A common assumption of the wavelet-based image interpolation approaches is that the input image is treated as the low frequency subbands of an unknown wavelet-transformed high-resolution image. Then the unknown high-resolution image can be reconstructed by estimating the wavelet coefficients of the high frequency subbands, followed by applying the inverse wavelet transform (Chang, Cvetkovic, & Vetterli, 1995; Temizel & Vlachos, 2006).

The challenge of conducting wavelet-based interpolation is to estimate the unknown wavelet coefficients of the high frequency subbands. The major widely-used approach is to exploit the inter-scale correlations between the high frequency wavelet coefficients and the low frequency subbsands using statistical models, particularly the *Gaussian mixture* (GM) model (Crouse, Nowak, & Baraniuk, 1998; Kim, Lee, & Cho, 2006; Kinebuchi, Muresan, & Parks, 2001; Woo, Eom, & Kim, 2004; Zhao, Han, & Peng, 2003). However, this GM model neglects the correlations among the sign information of the wavelet coefficients, since the Gaussian distribution is *symmetrical* around the zero (Temizel, 2007). Inaccurate estimation of the sign of wavelet coefficients could result in implausible artifacts in the reconstructed image. To justify this, a simulation is conducted using the *Lena* image. A one-level wavelet decomposition (using the well-known *Daubechies*-97 wavelets) is applied on the test image (shown in Fig. 1(a)), then the signs of all high frequency wavelet coefficients are changed, finally an inverse wavelet transform is applied to produce an image (shown in Fig. 1(b)). Comparing Fig. 1(a) and Fig. 1(b), one can see that the sign information of the wavelet coefficients has a critical role to control the quality of the reconstructed image.

To tackle the above challenge, a *three-component exponential mixture* (TCEM) model is proposed in this paper by formulating the probability distribution of individual wavelet coefficient using three components: (i) a Gaussian component, (ii) a positive exponential component, and (iii) a negative exponential component. Due to the fact that the exponential distribution is *not* symmetrical around the zero, the proposed model is able to exploit both the magnitude information and the sign information of the wavelet coefficients. Then, the proposed TCEM model is exploited to develop an image interpolation algorithm, by exploiting the inter-scale correlation between the low frequency wavelet coefficients and the high frequency wavelet coefficients.

There is a key fundamental issue that needs to be addressed for the proposed TCEM model; that is how to estimate the parameters of the proposed TCEM model. To tackle this issue, the *ant colony optimization* technique is used in this paper. The ACO technique is exploited to classify the wavelet coefficients into one of three

* Corresponding author.
E-mail address: eejtian@gmail.com (J. Tian).

0957-4174/$ - see front matter © 2011 Elsevier Ltd. All rights reserved.
doi:10.1016/j.eswa.2011.04.037

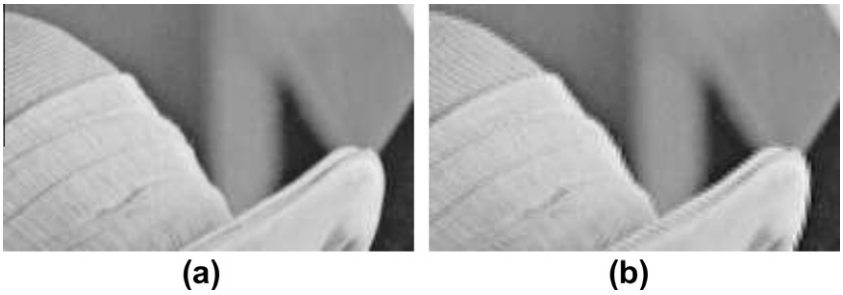

Fig. 1. (a) Original *Lena* image; (b) the reconstructed image, by applying one-level wavelet decomposition transform on the image (a) and changing the signs of high frequency wavelet coefficients, followed by applying the inverse wavelet transform.

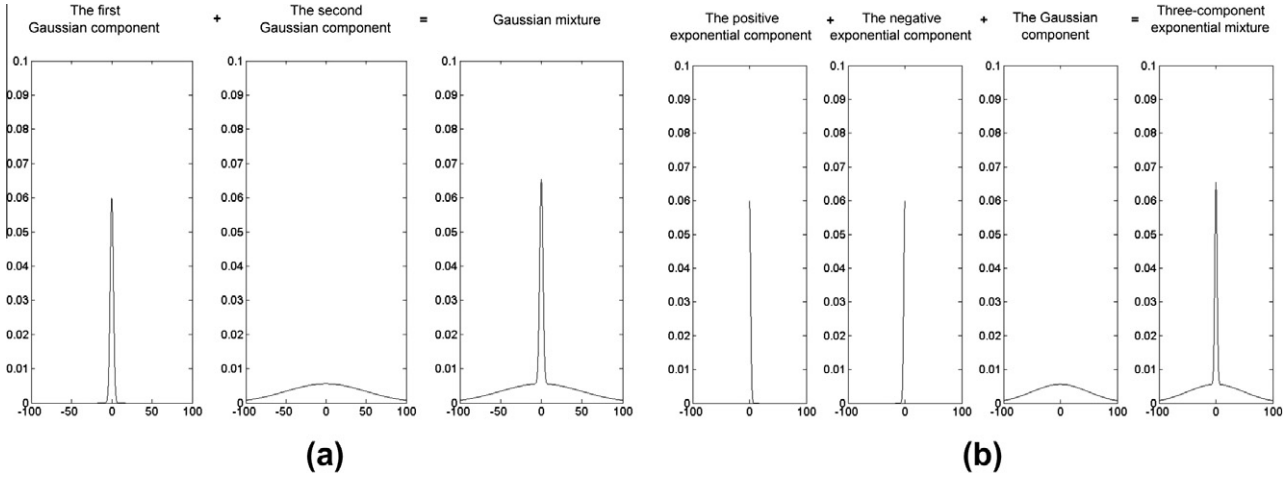

Fig. 2. A comparison between the two-component Gaussian mixture model (Crouse et al., 1998) and the proposed three-component exponential mixture model: (a) a two-component Gaussian mixture model consisting of two Gaussian components; and (b) the proposed three-component exponential mixture model consisting of three exponential components: a Gaussian component, a positive exponential component, plus a negative exponential component.

components of the proposed TCEM model, then estimate the parameters of each component. ACO is a nature-inspired optimization algorithm (Dorigo & Thomas, 2004) motivated by the natural collective foraging behavior of real-world ant colonies. Despite the fact that ACO has been widely applied to tackle numerous optimization problems (Dorigo, Gambardella, Middendorf, & Stutzle, 2002), its applications in image processing are quite a few (Hegarat-Mascle, Kallel, & Descombes, 2007; Malisia & Tizhoosh, 2006; Ouadfel & Batouche, 2003; Tian, Yu, & Xie, 2008b).

The rest of this paper is organized as follows. The proposed image interpolation approach is presented in Section 2 where a brief introduction to the conventional GM model and the proposed TCEM model is first provided, followed by estimating the parameters of the proposed TCEM model using the ACO technique. Extensive experimental results are presented in Section 3. Finally, Section 4 concludes this paper.

2. Proposed image interpolation approach

Basically, the idea of the proposed image interpolation approach is to treat the input image as the low frequency subbands of an unknown wavelet-transformed high-resolution image, and then produces the unknown high-resolution image by estimating the wavelet coefficients of the high frequency subbands. The proposed approach exploits the proposed TCEM model to formulate the statistical models of the low frequency subbands (i.e., the *known* low-resolution image), the parameters of which are estimated using the ACO technique. Then, the inter-scale correlation between the low frequency subbands and the high frequency subbands is exploited to estimate the statistical model of the coefficients of the *unknown* high frequency subbands. Finally, the coefficients of the high frequency subbands are synthesized via sampling from the above estimated model.

The key issues of the proposed approach boil down to the following three aspects: (i) build up the statistical model of the *known* wavelet coefficients, (ii) estimate the parameters of the above known statistical model, and (iii) estimate the model of the *unknown* wavelet coefficients using the inter-scale correlations among the wavelet coefficients. These three key issues are discussed in detail in the following subsections, respectively.

2.1. Statistical model of wavelet coefficients

2.1.1. Conventional Gaussian mixture model

A two-component *Gaussian mixture* (GM) model is developed in Crouse et al. (1998) for modeling the distribution of individual wavelet coefficients, as illustrated in Fig. 2(a). This is motivated by the fact that most wavelet coefficients of a natural image have small values and contain very little signal information; on the other hand, a few wavelet coefficients have large values that represent significant signal information. The above-mentioned characteristics can be mathematically formulated as follow. Denote the ith wavelet coefficient at the subband with the jth scale and kth direction as $S_i^{j,k}$. It has a distribution as

$$p\left(S_i^{j,k}\right) = q_i^{j,k} N\left(0, \sigma^2_{h_i^{j,k}}\right) + \left(1 - q_i^{j,k}\right) N\left(0, \sigma^2_{l_i^{j,k}}\right), \quad (1)$$

where $N(\mu,\sigma^2)$ represents a Gaussian distribution with a mean μ and a variance σ^2. Note that $\sigma_{h_i^{j,k}}$ is assumed to be larger than $\sigma_{l_i^{j,k}}$, without the loss of the generality.

2.1.2. Proposed three-component exponential mixture model

In contrast to the above-mentioned *two*-component Gaussian mixture model, a TCEM model is proposed in this paper, where the distribution of each individual wavelet coefficient contains *three* components; that is, a Gaussian component, a positive exponential component, and a negative exponential component, as illustrated in Fig. 2(b). To be more specific, denote the ith wavelet coefficient at the subband with the jth scale and kth direction as $S_i^{j,k}$, it has a distribution as

$$p\left(S_i^{j,k}\right) = a_i^{j,k}N\left(0,\sigma_i^{j,k}\right) + b_i^{j,k}E\left(\lambda_i^{j,k}\right) + c_i^{j,k}E\left(\lambda_i^{j,k}\right) \propto \frac{a_i^{j,k}}{\sigma_i^{j,k}}e^{-\frac{\left(s_i^{j,k}\right)^2}{2(\sigma_i^{j,k})^2}} + b_i^{j,k}\lambda_i^{j,k}e^{-\lambda_i^{j,k}s_i^{j,k}} + c_i^{j,k}\lambda_i^{j,k}e^{-\lambda_i^{j,k}s_i^{j,k}}, \quad (2)$$

where $a_i^{j,k}+b_i^{j,k}+c_i^{j,k}=1$, $N(\mu,\sigma)$ represents a Gaussian distribution with a mean μ and a standard derivation σ, $E(\lambda)$ represents an exponential distribution with a parameter λ. Due to the fact that the exponential distribution is *not* symmetrical around the zero, the proposed model is able to exploit both the magnitude information and the sign information of the wavelet coefficients.

2.2. Parameter estimation of the proposed TCEM model

The aim of this section is to estimate the parameters of the proposed TCEM model; that is $a_i^{j,k}, \sigma_i^{j,k}, b_i^{j,k}, \lambda_i^{j,k}, c_i^{j,k}$ at each location (i.e., the ith wavelet coefficient at the subband with the jth scale and kth direction). For that, two approaches that are used to estimate the parameters of the conventional GM model could be considered as the candidates. First, the *Expectation-Maximization* (EM) was used in Kinebuchi et al. (2001). However, this approach has a huge computational load and it cannot guarantee the global convergence, since it is relied on the initial solution. Second, Woo et al. proposed a deterministic approach to classify the wavelet coefficients into two categories using a threshold, then estimate their respective parameters (Kim et al., 2006). However, this approach neglects the intra-scale correlation among the wavelet coefficients and treats each wavelet coefficient independently.

To tackle the above problem, the ACO technique is used in this paper. The proposed approach first classifies each wavelet coefficient into one of three categories (i.e., three components of the proposed TCEM model), then estimates the parameters of each component. The proposed ACO-based approach aims to utilize a number of ants to move on a 2-D image for constructing a pheromone matrix, each entry of which represents certain feature at each pixel location of the image. Furthermore, the movements of the ants are steered by the amplitude information of the wavelet coefficient.

To be more specific, the proposed approach starts from assigning one ant on each subband of the image (with a size of $M_1 \times M_2$), each pixel of which can be viewed as a node. Furthermore, the initial value of each component of the pheromone matrix $\boldsymbol{\tau}^{(0)}$ is set to be a constant τ_{init}, which is experimentally set to be 0.0001 in our paper. Then the proposed algorithm runs for N iterations, in each iteration, each ant moves to neighboring coefficients and the pheromone content of the coefficient on the ant's path are updated. Finally, an image classification is performed at each wavelet coefficient by considering the normalized pheromone matrix, not the original amplitude value of the wavelet coefficient, using the K-means clustering algorithm (K is 3 in our context, since our aim is to classify each wavelet coefficient into three categories; that is three components of the proposed TCEM model).

There are two issues need to be addressed for the proposed approach: the ant movement and the pheromone update; both of which are presented in detail as follows.

- *Ant Movement*
  At the nth iteration, one ant is randomly selected, and this ant will consecutively move on the image for L movement-steps. This ant moves from the node (l,m) to its neighboring node (i,j) according to a transition probability that is defined as

$$p_{(l,m),(i,j)}^{(n)} = \frac{\left(\tau_{i,j}^{(n-1)}\right)^{\alpha}(\eta_{i,j})^{\beta}}{\sum_{(i,j)\in\Omega_{(l,m)}}\left(\tau_{i,j}^{(n-1)}\right)^{\alpha}(\eta_{i,j})^{\beta}}, \quad (3)$$

  where $\tau_{i,j}^{(n-1)}$ is the pheromone value of the node (i,j), $\Omega_{(l,m)}$ is the neighborhood nodes of the node (l,m), $\eta_{i,j}$ represents the heuristic information at the node (i,j). The constants α and β represent the influence of the pheromone matrix and the heuristic matrix, respectively; they are experimentally set to be $\alpha = 1$, $\beta = 2$, respectively.
  There are two crucial issues in the construction process. The first issue is the determination of the heuristic information $\eta_{i,j}$ in (3). In this paper, it is proposed to be determined by the local statistics at the pixel position (i,j) as the inverse of the absolute value of the difference between the wavelet coefficient (i,j) and the mean of the current path. The second issue is to determine the permissable range of the ant's movement (i.e., $\Omega_{(l,m)}$ in (3)) at the position (l,m). In this paper, it is proposed to be 8-connectivity neighborhood.
- *Pheromone Update*
  The proposed approach performs two updates operations for updating the pheromone matrix.
  - The first update is performed after the movement of each ant within each construction-step. Each component of the pheromone matrix is updated according to

$$\tau_{i,j}^{(n-1)} = \begin{cases} (1-\rho)\cdot\tau_{i,j}^{(n-1)} + \rho\cdot\Delta_{i,j}^{(k)}, & \text{if } (i,j) \text{ is visited by the current } k\text{th ant;} \\ \tau_{i,j}^{(n-1)}, & \text{otherwise,} \end{cases} \quad (4)$$

    where ρ is experimentally selected to be 0.1 in our simulations, $\Delta_{i,j}^{(k)}$ is determined by the heuristic matrix; that is, $\Delta_{i,j}^{(k)} = \frac{1}{|\eta_{i,j}|}$.
  - The second update is carried out after the movement of all ants within each construction-step according to

$$\boldsymbol{\tau}^{(n)} = (1-\psi)\cdot\boldsymbol{\tau}^{(n-1)} + \psi\cdot\boldsymbol{\tau}^{(0)}, \quad (5)$$

    where ψ is the *pheromone decay coefficient*, which is experimentally selected to be 0.3.

A summary of the implementation of the proposed approach is presented in Fig. 3. The proposed approach starts from the initialization process, and then runs for N iterations to construct the pheromone matrix by performing both the construction process and the update process. Finally, the category of each wavelet coefficient is determined according to the above-constructed pheromone matrix.

After applying the ACO technique to classify each wavelet coefficient into the three categories (i.e., three components of the proposed TCEM model), the parameters are estimated as follows. The mixture parameter $a_i^{j,k}$ is defined as the ratio between the number of the neighboring coefficients (classified into the Gaussian component) of $S_i^{j,k}$ and the total number of neighboring coefficients of $S_i^{j,k}$ (imposed by a square-shaped $M \times M$ window on the coefficient $S_i^{j,k}$). Furthermore, $\sigma_i^{j,k}$ is defined as the standard derivation of these

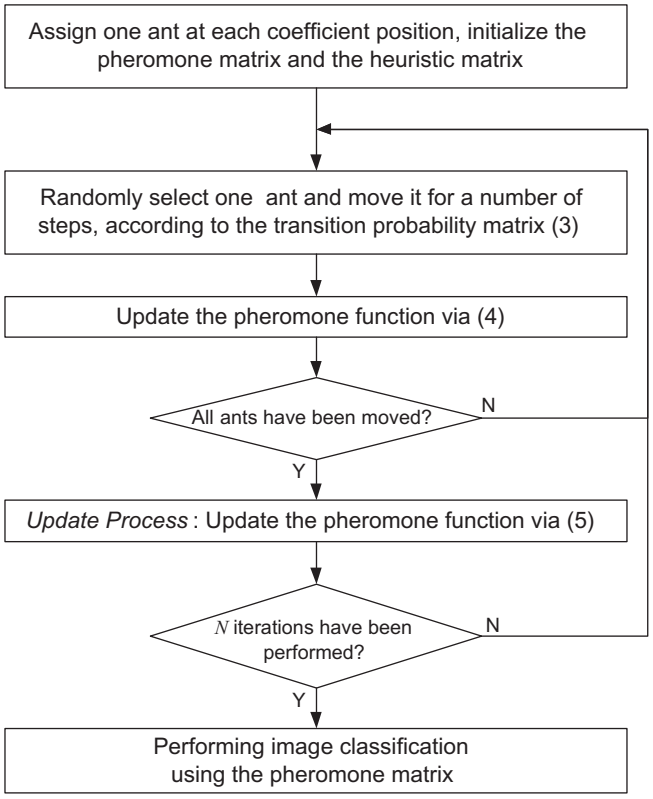

Fig. 3. A summary of the implementation of the proposed ACO-based image classification approach.

coefficients. Similarly, the neighboring coefficients that belong to the positive and negative exponential components are used to estimate their respective parameters $b_i^{j,k}, \lambda_i^{j,k}, c_i^{j,k}$.

2.3. Inter-scale correlation of wavelet coefficients

In order to estimate the unknown high frequency wavelet coefficients, their statistical model needs to be estimated by applying the inter-scale correlation on the statistical model estimated from the low frequency wavelet coefficients. The inter-scale correlation relationship used in this paper was developed in our earlier work (Tian, Yu, & Xie, 2008a); it is briefly presented as below. First, the variance of the wavelet coefficients are exponentially decayed through the scale of the wavelet subbands. More specifically, considering the variance parameter of the coefficient $\sigma_i^{j,k}$, the relationship between it and its parent and child coefficients $\sigma_i^{j+1,k}$ and $\sigma_{h_i^{j-1,k}}$ can be formulated as Tian et al. (2008a)

$$\frac{\sigma_i^{j+1,k}}{\sigma_i^{j,k}} = \frac{\sigma_i^{j,k}}{\sigma_i^{j-1,k}}. \tag{6}$$

Similar relationship is applied for the parameter of the exponential components of the proposed TCEM model; that is Tian et al. (2008a)

$$\frac{\lambda_i^{j+1,k}}{\lambda_i^{j,k}} = \frac{\lambda_i^{j,k}}{\lambda_i^{j-1,k}}. \tag{7}$$

Secondly, the persistence of large or small wavelet coefficient magnitudes becomes exponentially stronger at finer scale; that is, the relationship between the probability of the coefficient (i.e. $a_i^{j,k}, b_i^{j,k}$ and $c_i^{j,k}$) and that of its parent coefficient (i.e., $a_i^{j+1,k}, b_i^{j+1,k}$ and $c_i^{j+1,k}$) is Tian et al. (2008a)

$$\begin{pmatrix} P\left(a_i^{j,k} = \tau_i^{j,k}\right) \\ P\left(b_i^{j,k} = \tau_i^{j,k}\right) \\ P\left(c_i^{j,k} = \tau_i^{j,k}\right) \end{pmatrix} = \begin{pmatrix} 1 & 1/2 & 1/2 \\ 0 & 1/4 & 1/4 \\ 0 & 1/4 & 1/4 \end{pmatrix} \cdot \begin{pmatrix} P\left(a_i^{j+1,k} = \tau_i^{j+1,k}\right) \\ P\left(b_i^{j+1,k} = \tau_i^{j+1,k}\right) \\ P\left(c_i^{j+1,k} = \tau_i^{j+1,k}\right) \end{pmatrix}, \tag{8}$$

where $\tau_i^{j+1,k} = \max\left(a_i^{j+1,k}, b_i^{j+1,k}, c_i^{j+1,k}\right)$.

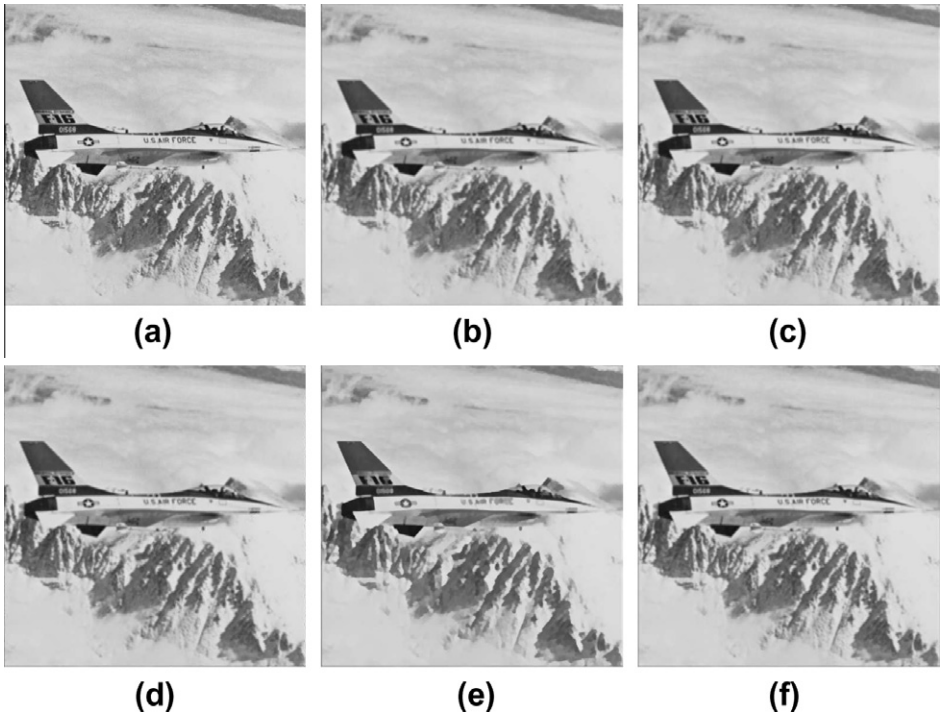

Fig. 4. The subjective performance comparison: (a) the original *Airplane* image; (b) simulated low-resolution image; (c) bi-linear interpolation (PSNR = 28.00 dB); (d) Li and Orchard's approach (Li & Orchard, 2001) (PSNR = 29.16 dB); (e) Woo et al.'s approach (Woo et al., 2004) (PSNR = 29.35 dB); (f) proposed approach (PSNR = 29.84 dB).

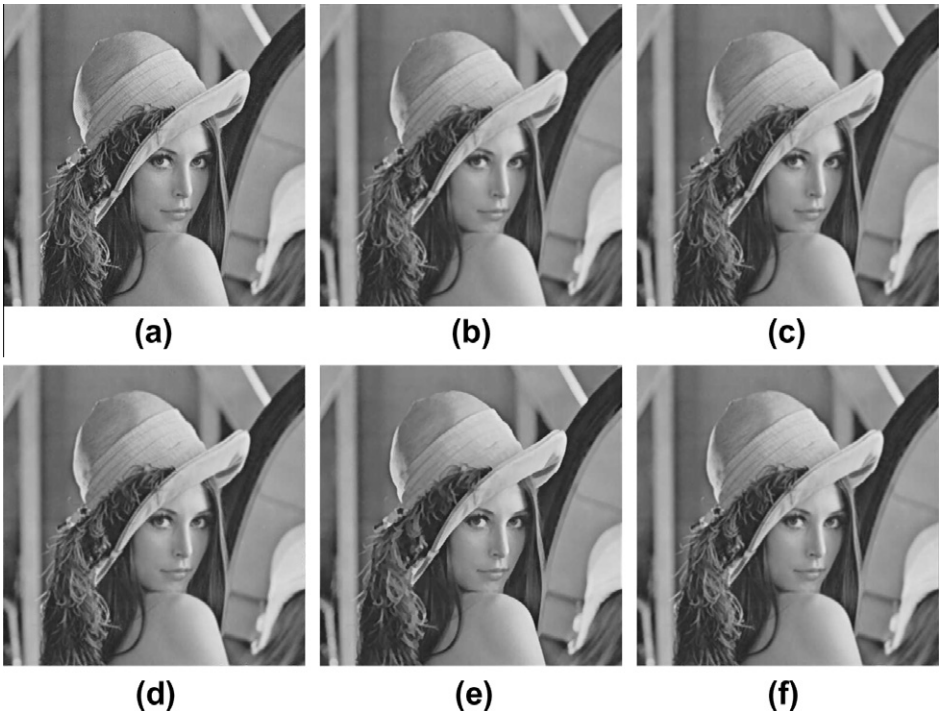

Fig. 5. The subjective performance comparison: (a) the original *Lena* image; (b) simulated low-resolution image; (c) bi-linear interpolation (PSNR = 29.78 dB); (d) Li and Orchard's approach (Li & Orchard, 2001) (PSNR = 31.88 dB); (e) Woo et al.'s approach (Woo et al., 2004) (PSNR = 31.60 dB); (f) proposed approach (PSNR = 32.28 dB).

2.4. Summary of the proposed image interpolation approach

A summary of the proposed image interpolation approach is provided as below.

- Firstly, a J-level wavelet decomposition is applied on the input low-resolution image.
- The proposed TCEM model is used to formulate the statistical distribution of the above J-level wavelet coefficients as mentioned in Section 2.1, and the model parameters of the proposed TCEM model are estimated using the ACO technique as mentioned in Section 2.2.
- The distribution of the desired high-pass filtered wavelet coefficient in the 0th level subband is estimated via (7) and (8) as mentioned in Section 2.3, and then generate the 0th level wavelet coefficients via (2).
- Finally, the $(J+1)$-level inverse wavelet transform is applied to produce the final reconstructed image.

3. Experimental results

The first experiment is to explore the performance of the proposed approach using gray test images *Airplane* and *Lena*, which serve as the ground truth and compared with the reconstructed images for performance comparison. In our simulation, the observed low-resolution images are independently generated by convolving each ground truth image with a point spread function, which is an average low-pass filter with a size of 3×3, followed by a down-sampling operation with a ratio 2 in both horizontal and vertical directions, respectively.

The proposed wavelet-based interpolation approach performs image interpolation using the *Daubechies*-97 wavelets with three levels decomposition. Then the high-pass filtered coefficients are estimated as presented in Section 2.4. Finally, the inverse wavelet transform is applied to obtain the reconstructed image. Since the coefficients of the high frequency subbands need to be synthesized via sampling from the above estimated model, they will differ for each simulation. Therefore, one hundred simulations are run and their average are reported as the final reconstructed image.

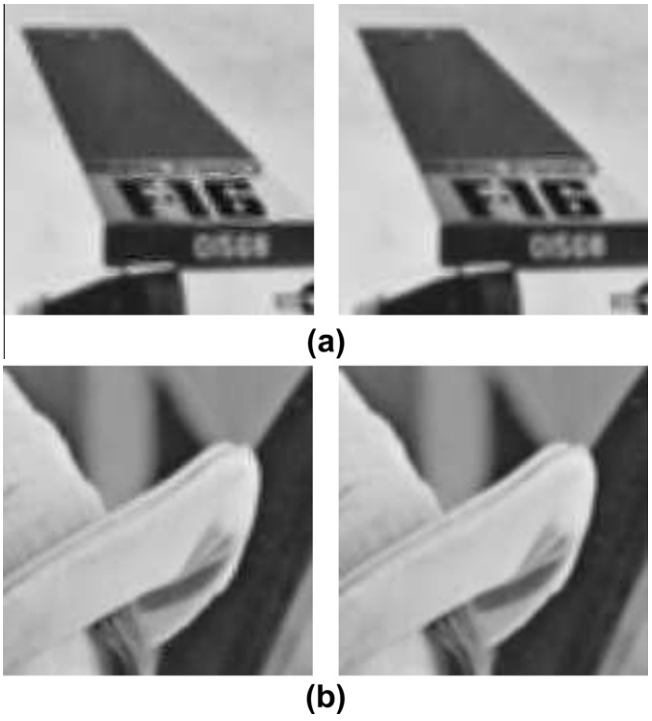

Fig. 6. Close-up performance comparison of gray images: (a) Woo et al.'s approach (Woo et al., 2004); (b) proposed approach.

Table 1
The PSNR performance comparison.

Test image	Bi-linear interpolation	Li and Orchard's approach (Li & Orchard, 2001)	Woo et al.'s approach (Woo et al., 2004)	Krylov and Nasonov's approach (Krylov & Nasonov, 2008)	Proposed approach
Airplane	28.00 dB	29.16 dB	29.35 dB	29.21 dB	29.84 dB
Lena	29.78 dB	31.88 dB	31.60 dB	31.71 dB	32.28 dB

Table 2
The PQS (Miyahara et al., 1998) performance comparison.

Test image	Bi-linear interpolation	Li and Orchard's approach (Li & Orchard, 2001)	Woo et al.'s approach (Woo et al., 2004)	Krylov and Nasonov's approach (Krylov & Nasonov, 2008)	Proposed approach
Airplane	36.83 dB	41.14 dB	42.56 dB	40.34 dB	42.87 dB
Lena	38.25 dB	43.42 dB	44.90 dB	43.58 dB	45.37 dB

Furthermore, the parameters of the proposed ACO-based classification approach are experimentally set as follows: $L = 15$,$N = 5$, and $M = 5$.

Experiments are conducted to compare the performance of the proposed approach with that of *bi-linear interpolation* and three interpolation algorithms developed in Li and Orchard (2001), Woo et al. (2004) and Krylov and Nasonov (2008), respectively. To provide the objective performance comparison, two image quality measurements are used in this paper; that is, *PSNR* and *picture quality scale* (PQS) (Miyahara, Kotani, & Algazi, 1998). They are defined as follows. Let $x_{i,j}$ and $y_{i,j}$ denote the pixels at the position (i,j) of the original (i.e., the ground truth) image and the reconstructed image with a size of $M_1 \times M_2$ each, respectively. Firstly, the PSNR is defined as

$$PSNR = 10 \cdot log_{10} \frac{Q^2}{\frac{1}{M_1 \times M_2} \sum_{i=1}^{M_1} \sum_{j=1}^{M_2} (x_{i,j} - y_{i,j})^2}, \quad (9)$$

where $Q = 255$ for 8-bit gray images. Secondly, the PQS (Miyahara et al., 1998) computes the weighted difference between x and y, where the weighting function $f(\cdot)$ represents the frequency-selective property of the human visual system; that is, *PQS* yields the form as Miyahara et al. (1998)

$$PQS = 10 \cdot log_{10} \frac{1}{\frac{1}{M_1 \times M_2} \sum_{i=1}^{M_1} \sum_{j=1}^{M_2} (f(x_{i,j} - y_{i,j}))^2}, \quad (10)$$

where the function $f(\cdot)$ is defined as same as that of Miyahara et al. (1998). A larger PQS value indicates a better image quality. Tables 1 and 2 compare their PSNR and PQS (Miyahara et al., 1998) performances, respectively; and Figs. 4–6 present various image results of the above four algorithms. As seen from the above tables and figures, the proposed algorithm always yields the best performance among the above-mentioned four algorithms.

4. Conclusions

A three-component exponential mixture model has been successfully proposed in this paper to develop a wavelet-based image interpolation approach. Due to the fact that the exponential distribution is *not* symmetrical around the zero, the proposed model is able to exploit both the magnitude information and the sign information of the wavelet coefficients. Consequently, the proposed approach can effectively exploit the correlation among the low-pass filtered wavelet coefficients and the high-pass filtered wavelet coefficients to yield superior interpolated image result, as verified in our extensive experimental results. Furthermore, the ACO technique has been exploited to perform parameter estimation of the proposed approach.

There are several directions that could be considered for future research. First, the proposed approach is independently applied for each high-pass filtered subband of the noisy image. It could be further improved by considering the inter-scale correlation among the wavelet coefficients (Sendur & Selesnick, 2002) to perform classifying. Second, the parallel ACO algorithm (Randall & Lewis, 2002) can be exploited to further reduce the computational load of the proposed image classification algorithm; consequently, shorten the execution time of the proposed approach.

Acknowledgements

This work was supported by the National Natural Science Foundation of China (60872123, 60972133); GDSF Team Project (9351064101000003); the Joint Fund of the National Natural Science Foundation and the Guangdong Provincial Natural Science Foundation (U0835001); the Fundamental Research Funds for the Central Universities (x2dxD2105260), SCUT; Fund of Provincial Key Lab for Computer Information Processing Tech. (No. KJS0922).

References

Chang, S. G., Cvetkovic, Z., & Vetterli, M. (1995). Resolution enhancement of images using wavelet transform extrema extrapolation. In *Proceedings of the IEEE international conference on acoustics, speech, signal processing, Detroit, MI, May* (pp. 2379–2382).

Crouse, M. S., Nowak, R. D., & Baraniuk, R. G. (1998). Wavelet-based statistical signal processing using hidden Markov models. *IEEE Transactions on Signal Processing, 46*(April), 886–902.

Dorigo, M., Gambardella, L. M., Middendorf, M., & Stutzle, T. (2002). Special issue on ant colony optimization. *IEEE Transactions on Evolutionary Computation, 6*(July).

Dorigo, M., & Thomas, S. (2004). *Ant colony optimization*. Cambridge: MIT Press.

Hegarat-Mascle, S. L., Kallel, A., & Descombes, X. (2007). Ant colony optimization for image regularization based on a nonstationary Markov modeling. *IEEE Transactions on Image Processing, 16*(March), 865–878.

Kim, J. H., Lee, S. H., & Cho, N. I. (2006). Bayesian image interpolation based on the learning and estimation of higher bandwavelet coefficients. In *Proceedings of the IEEE international conference on image processing, Atlanta, GA, October* (pp. 685–688).

Kinebuchi, K., Muresan, D. D., & Parks, T. W. (2001). Image interpolation using wavelet-based hidden Markov trees. In *Proceedings of the IEEE international conference on acoustic, speech and signal processing, Salt Lake City, UT, May* (pp. 7–11).

Krylov, A., & Nasonov, A. (2008). Adaptive total variation deringing method for image interpolation. In *IEEE International conference on image processing, San Diego* (pp. 2608–2611).

Li, X., & Orchard, M. (2001). New edge-directed interpolation. *IEEE Transactions on Image Processing, 10*(October), 1521–1527.

Malisia, A. R., & Tizhoosh, H. R. (2006). Image thresholding using ant colony optimization. In *Proceedings Canadian conference on computer and robot vision, Quebec, Canada, June* (pp. 26–31).

Miyahara, M., Kotani, K., & Algazi, V. R. (1998). Objective picture quality scale (PQS) for image coding. *IEEE Transactions on Communications, 46*, 1215–1226.

Ouadfel, S., & Batouche, M. (2003). Ant colony system with local search for Markov random field image segmentation. In *Proceedings of the IEEE international conference on image processing, Barcelona, Spain, September* (pp. 133–136).

Randall, M., & Lewis, A. (2002). A parallel implementation of ant colony optimization. *Journal of Parallel and Distributed Computing, 62*, 1421–1432.

Sendur, L., & Selesnick, I. W. (2002). Bivariate shrinkage with local variance estimation. *IEEE Signal Processing Letters, 9*, 438–441.

Temizel, A. (2007). Image resolution enhancement using wavelet domain hidden Markov tree and coefficient sign estimation. In *Proceedings of the IEEE international conference on image processing, San Antonio, TX, September* (pp. 381–384).

Temizel, A., & Vlachos, T. (2006). Wavelet domain image resolution enhancement. *IEE Proceedings-Vision, Image and Signal Processing, 153*, 25–30.

Tian, J., Yu, W.-Y., & Xie, S.-L. (2008). Wavelet-based image interpolation using a three-component exponential mixture model. In *Proceedings of the international congress on image and signal processing, Sanya, China, May* (pp. 129–132).

Tian, J., Yu, W., & Xie, S. (2008). An ant colony optimization algorithm for image edge detection. In *Proceedings of the IEEE congress on evolutionary computation, Hongkong, China, June* (pp. 751–756).

Woo, D. H., Eom, I. K., & Kim, Y. S. (2004). Image interpolation based on inter-scale dependency in wavelet domain. In *Proceedings of the IEEE international conference on image processing, Singapore, September* (pp. 1687–1690).

Zhao, S., Han, H., & Peng, S. (2003). Wavelet domain HMT-based image superresolution. In *Proceedings of the IEEE international conference on image processing, Barcelona, Spain* (pp. 953–956).